Available online at www.sciencedirect.com
SCIENCE DIRECT®
C. R. Physique 4 (2003) 163–173
COMPTES RENDUS PHYSIQUE

Optical telecommunications/Les télécommunications optiques

All-optical signal regeneration: from first principles to a 40 Gbit/s system demonstration

Régénération tout-optique du signal : des principes aux démonstrations de systèmes à 40 Gbit/s

Olivier Leclerc *, Bruno Lavigne, Elodie Balmefrezol, Patrick Brindel, Laurent Pierre, Delphine Rouvillain, Frederic Seguineau

Alcatel Research & Innovation, route de Nozay, 91461 Marcoussis cedex, France

Received 14 October 2002

Presented by Guy Laval

Abstract

As optical amplifiers have opened new perspectives for optical communication systems with ultra-high capacities and long-haul transmission distances (more than 1 Tbit/s over 10 000 km), fundamental limits are being reached. In order to overcome these propagation impairments, another technology revolution is soon required. Promising developments concern in-line all-optical regeneration, which makes it possible to transmit optical data over virtually unlimited distances. In this article, we recall the basic principle of Optical Regeneration in optical communication systems and review the current technology alternatives foreseen for future 40 Gbit/s transmission system implementation. The alternative offered by opto-electronic regeneration is also discussed, as to identify and highlight the advantages of the all-optical approach. ***To cite this article: O. Leclerc et al., C. R. Physique 4 (2003).***

Résumé

L'avènement des amplificateurs optiques ayant ouvert de nouvelles perspectives pour les systèmes de communications optiques ultra longue distance et à ultra grande capacité (plus d'un Terabit/s sur 10 000 km), des limites fondamentales semblent aujourd'hui être atteintes. Afin de s'affranchir partiellement des dégradations du signal ayant trait à la propagation, une révolution technologique est devenue nécessaire. A ce titre, les techniques de régénération optique du signal en ligne permettant la transmission de données en optique sur des distances virtuellement infinies ont fait l'objet de récents développements prometteurs. Dans cet article, nous introduirons les principes de base de la Régénération Optique dans les systèmes optiques et nous détaillerons les différentes technologies envisagées pour son implantation dans les futurs systèmes de transmission à 40 Gbit/s. La solution offerte par la régénération opto-électronique sera aussi abordée afin notamment d'identifier et de mettre en avant les avantages des approches tout-optiques. ***Pour citer cet article : O. Leclerc et al., C. R. Physique 4 (2003).***

Keywords: Optical communications; Optical regeneration; Optical signal processing; Optical gates; All-optical devices; Nonlinear optics; Semiconductor components; Interferometers; Optical solitons

* Corresponding author.
E-mail address: Olivier.Leclerc@alcatel.fr (O. Leclerc).

1631-0705/03/$ – see front matter
doi:10.1016/S1631-0705(03)00007-0

Mots-clés : Communications optiques ; Régénération optique ; Traitement tout-optique du signal ; Portes optiques ; Dispositifs tout-optiques ; Optique non-linéaire ; Composants à semiconducteurs ; Interferomètres ; Solitons optiques

1. Introduction

The breakthrough of optical amplification combined with the techniques of *Wavelength-Division Multiplexing* (WDM) and *dispersion management* have made it possible to exploit a sizeable fraction of the optical fiber bandwidth (several terahertz). Systems based on 10 Gbit/s per channel bit-rate and showing capacities of several terabit/s with transmission capabilities of hundreds to thousands of kilometers have reached the commercial area.

While even greater capacities and bit-rate/bandwidth efficiencies could be reached with current technologies, there is potential economic interest in reducing the number of wavelength-channels by increasing the channel rate (e.g., 40 Gbit/s). However, such an increase in the channel rate results in significant increases in transmission impairments, stemming from the combined effects of noise accumulation, fiber dispersion, fiber nonlinearity, leading to two main types of signal degradation. The first is concerns the *amplitude* domain; the power of marks (‘1’) and spaces (‘0’) randomly fluctuate because of interactions between signal and *amplified spontaneous emission* (ASE) noise or between channels through *cross-phase modulation* (XPM) combined with chromatic dispersion. The second concerns the *time* domain; the pulse time position randomly fluctuates (timing jitter) due to interactions between signal and ASE combined with dispersion. Preserving a high contrast between ‘1’ and ‘0’ powers and keeping amplitude/time fluctuations at low levels are mandatory to achieve high transmission quality, as measured *through bit-error-rate* (BER) or *Q-factors*.

To further increase system transmission distance or quality, two approaches exist. The first consists in segmenting the system into independent trunks interfaced by electronic repeater/transceivers. We shall refer to this approach as *opto-electronic (OE) regeneration*. The second approach is to implement *in-line all-optical signal regeneration*. It performs the same signal-restoring functions as in the OE solution, but with reduced complexity, band-limited electronics, higher optical bandwidth and enhanced capabilities.

Both OE and all-optical regeneration involve three basic signal-processing function, namely *re-amplifying, re-shaping* and *re-timing*, hence the generic acronym ‘3R’ (Fig. 1). Thus optical amplification provides a mere ‘1R’ signal-processing function. When there is no re-timing (usually referred to as ‘2R’), regeneration has only re-amplifying and re-shaping capabilities. Full 3R regeneration with retiming thus requires *clock recovery* (CR), which can be done either electronically or all-optically, as shown below. It should be noted that optical 3R is not necessarily void of electronic functions (e.g., when using electronic CR and OE modulation), but the main feature is that these electronic functions are band-limited (as opposed to broadband in the case of OE regeneration).

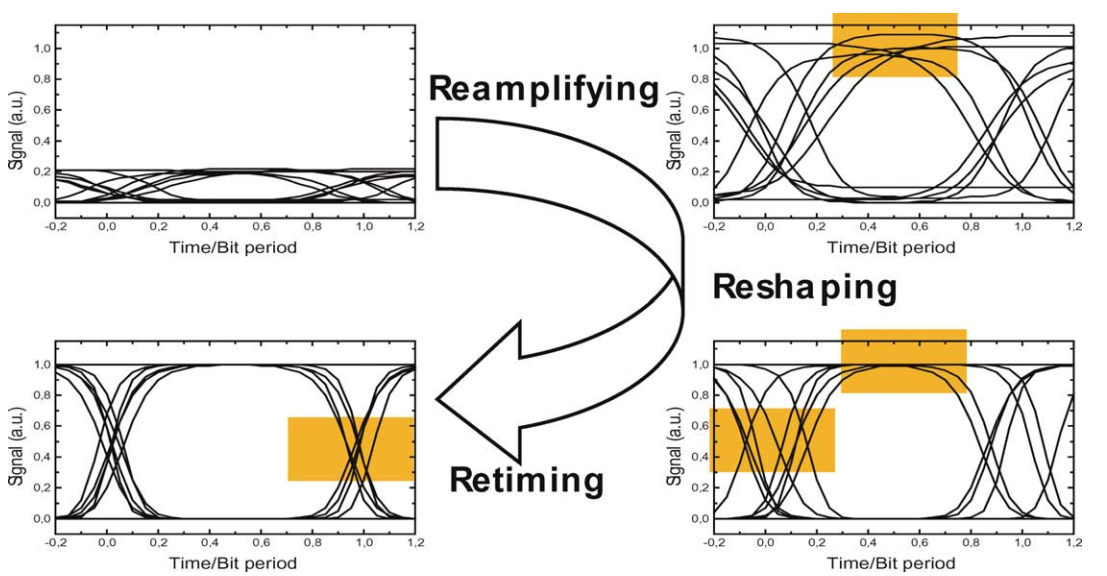

Fig. 1. Principle of 3R regeneration, as applied to NRZ signals: (1) Re-amplifying; (2) Re-shaping; and (3) Re-timing.

This paper reviews current technology alternatives for all-optical regeneration, considering both theoretical/experimental performance and practical implementation issues. Section 2 focuses on regeneration techniques using *nonlinear gates*, namely based upon *semiconductor optical amplifiers* (SOA) and *saturable absorbers* (SA). Section 3 concerns regeneration techniques based on *synchronous modulation*, while Section 4 discusses the issue of OE versus all-optical regeneration and the engineering/economical implications of the two approaches for high-capacity WDM systems.

2. Optical regeneration using nonlinear gates

We consider first optical regeneration based on *nonlinear optical gates*. A nonlinear gate can be defined as a three-port device where the second input port is used by a 'decision' control, such as in SOA gates. It can also be a two-port device, where the input signal acts as its own control, such as in SA gates.

Fig. 2 shows the generic layout of a 3R regenerator based on nonlinear gates. The noisy signals to be regenerated are first launched into the Re-amplification block. Part of the output signal is extracted in order to recover a synchronized clock signal, while the remnant is fed to the decision block, for simultaneous Re-shaping and Re-timing. Optimized regenerator design requires the adaptation of optical properties between all function-block features. The Re-amplification stage is not only a passive input-power adapter; it can also reduce intensity fluctuations (as caused by propagation or crossing routing/switching nodes), so as to provide the next stages with fixed input conditions. In this case, the Re-amplification block acts as an adaptation interface, suppressing input fluctuations in power, wavelength, polarization state or adapting possible changes in data format. In practice, this results in the addition in the Re-amplification block of a control circuitry (either optical or electrical) whose complexity directly depends on actual system environment (ultra-fast power equalization for packet-switching applications and compensation of slow power fluctuations in transmission applications).

The CR block provides a low-jitter, optical clock signal, as synchronized to the input data. Regardless of the CR technique (electronic or optical), the clock-pulse temporal width should match the decision window of the switching element. Hence, control of the optical clock pulse width is required for optimized operation of the second block. Therefore, sinusoidal clocks are not necessarily best suited. CR should also be adapted to system constraints. For instance, the introduction of optical packet-switching imposes new synchronization schemes with a-synchronism at bit level.

The end block, the decision gate, performs Re-shaping and Re-timing, and is the regenerator's core element. Ideally, it should also act as a transmitter capable of renewing or restoring optical pulse shapes. The chirp possibly introduced by the decision gate in the resulting signal should adequately match line transmission requirements.

In the following Section 2.1, we describe current solutions to realize the two main building blocks of all-optical regenerators: the decision and the CR elements. The issue of characterization and performance evaluation is also addressed. In Section 2.2 we then describe and actual implementation and system validation of a 40 Gbit/s optical 3R regenerator using an SOA-based device.

2.1. Building blocks of optical 3R regenerators

2.1.1. Decision element

As mentioned above, a key element of optical regenerators is the *nonlinear gate*, which performs the decision in the optical domain. Such gates have been extensively investigated and almost all of them are *optical interferometers*. This type of decision element uses either fiber-based or monolithic SOA-based devices, as seen below. The principle of operation is the following.

Consider an optical interferometer including one arm incorporating a nonlinear medium, as shown in Fig. 3(a). Assuming the presence of two signals: an input signal carried by λ_1 wavelength acting as a command and a local cw signal carried by λ_2 wavelength acting as a probe, the output power is given by:

$$P_{\text{out}}(\lambda_2)\alpha P_{\text{cw}}(\lambda_2)\left[1+\cos(\Delta\Phi P_{\text{in},\lambda_1})\right], \tag{1}$$

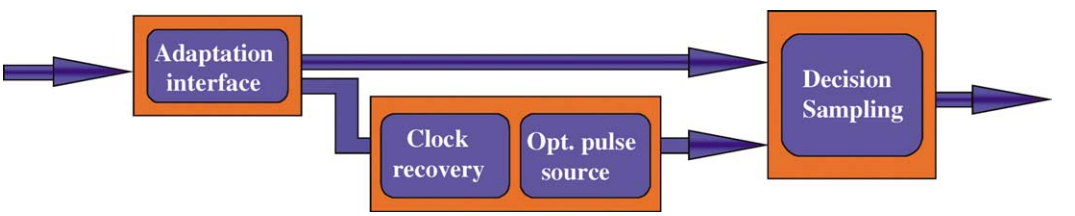

Fig. 2. Generic layout of 3R regenerator.

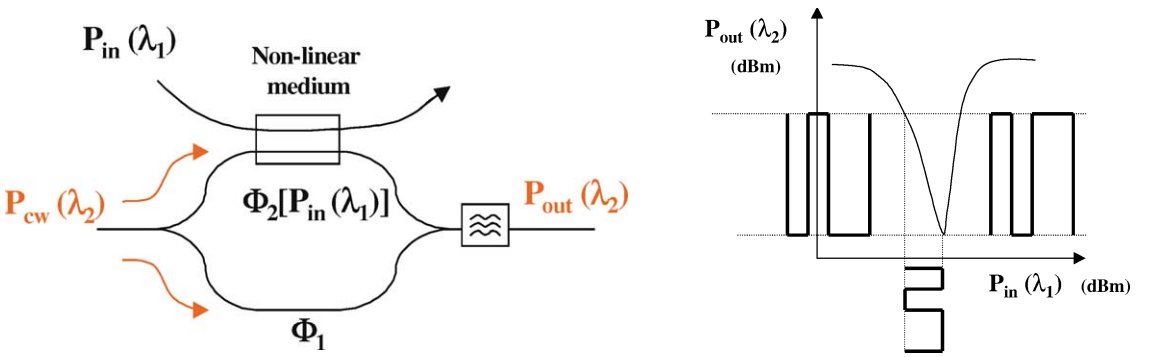

(a) (b)

Fig. 3. (a) Schematic of an optical interferometer with a nonlinear medium on one arm; (b) nonlinear transfer function of the interferometer and application to incident coded signals.

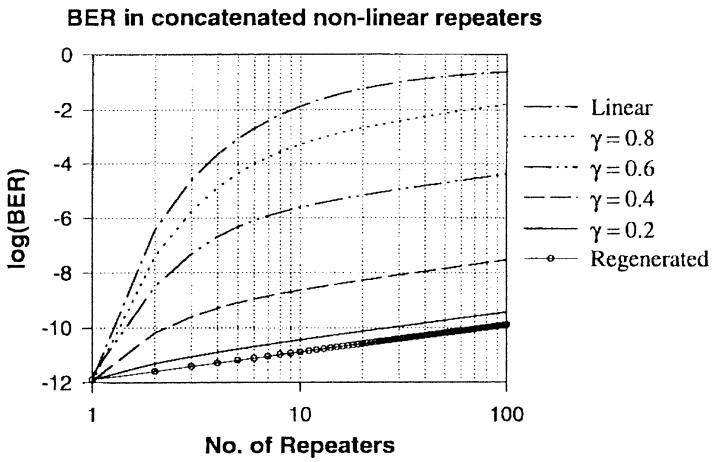

Fig. 4. Evolution of the BER with concatenated regenerators for different nonlinear transfer function (i.e., γ parameter). (Published with permission of the IEEE.)

where $\Delta\Phi(P_{\text{in},\lambda_1}) = \Phi_2(P_{\text{in},\lambda_1}) - \Phi_1$. Injection of the signal at λ_1 induces a phase shift through XPM, the amount of which depending upon power level P_{in,λ_1}. In turn, phase modulation (PM) induces amplitude modulation (AM) on the signal at λ_2. Fig. 3(b) shows the nonlinear transfer function of the interferometer. The fast nonlinearity induces noise redistribution, resulting in a narrower distribution for marks and spaces and improvement in the signal extinction ratio. Under these conditions, the interferometer performs as a 2R regenerator. Depending on the selected function slope, data polarity is preserved (positive slope) or switched (negative slope). It should be noted that if a pulsed-clock signal is substituted to the cw signal at λ_2, Re-shaping and Re-timing are simultaneously performed by the sampling effect, resulting in full 3R regeneration.

As we shall see below, the degree of nonlinearity in the decision's response reflects its regenerative properties. The theoretical evolution of BER with number of concatenated regenerators, for regenerators having different nonlinear responses, illustrates this feature in Fig. 4 [1]. The degree of nonlinearity is characterized through the factor γ which changes the shape of the non-linearity response from a step function ($\gamma = 0$) to a linear function ($\gamma = 1$). The noise level is adjusted so that the output BER is fixed to 10^{-12} after a single regenerator. As seen in Fig. 4, all curves standing for different regeneration efficiencies pass through a common point defined after the first device. This clearly indicates that it is not possible to qualify the regenerative capability of immediately at the output. Indeed, the BER is the same for either a 3R regenerator or a mere amplifier if only measured after a single element. The origin of this comes from the initial overlap between noise distributions associated to marks and spaces, that cannot be suppressed but only minimized by a single decision element through threshold adjustment. From Fig. 4, one observes different behaviors depending on the nonlinear function shape. The best regeneration performance is obtained with an ideal step function ($\gamma = 0$). In that case, BER linearly increase (i.e., more errors) in the cascade. Conversely, when nonlinearity is reduced (increasing γ), both BER and noise accumulate until the concatenation of nonlinear functions is reaching some steady-state pattern, from which BER linearly increases.

Concatenating of nonlinear devices thus magnifies shape differences in their nonlinear response. In practice, the experimental investigation of regenerator cascades is conducted in a re-circulating loops. After a few loop re-circulations (laps) a cumulative effect of all transmission impairments, such as chromatic dispersion, timing jitter and amplifier noise, is obtained, thus revealing the regenerative performance of the device under test.

In the physical domain, decision elements with ideal step response do not exist. Different nonlinear optical transfer functions approaching more or less the ideal can be realized in various media such as fiber, SOA, electro-absorption modulator (EAM), and laser. As previously stated, however, the most promising and flexible devices are interferometers, which can be classified according to the nature of the nonlinearity exploited to achieve a π-phase shift.

In the case of fiber-based devices such as the nonlinear optical loop mirror (NOLM), the phase shift is induced through Kerr effect in an optical fiber. The key advantage of fiber-based devices such as NOLM lies in the near-instantaneous (fs) response of the Kerr nonlinearity, making them very attractive for ultra-high bit-rate operation ($\geqslant$160 Gbit/s). On the negative side, major limitations come from environmental instability, strong polarization dependence and reduced integrability, mainly due the requirement of relatively long (km) fiber lengths. Polarization-insensitive NOLMs have been realized, although with the same drawbacks concerning integrability. A comprehensive overview of NOLM potentialities for all-optical signal processing and 3R regeneration is given in [2]. With recent development in highly nonlinear fibers, however, the required NOLM fiber length could be significantly reduced, hence dramatically reducing environmental instability.

A second type of device to consider is the integrated SOA-based, Mach–Zehnder interferometers (MZI). In MZIs, the phase shift is due to the effect of photo-induced carrier depletion in the gain saturation regime of one of the SOAs [3]. A phase shift of π can be produced by only 5 dB gain modulation. Control and probe can be launched in counter- or co-directional ways. In the first case, no optical filter is required at the output of the device for rejecting the signal at λ_1 wavelength but operation of the MZI is limited in speed.

At this point, one should mention that the photo-induced modulation effects in SOAs are intrinsically limited in speed by the gain recovery time, which is a function of the carrier lifetime and the injection current. An approach referred to as *differential operation mode* (DOM), which takes advantage of the MZI's interferometric properties, makes possible to increase speed up to 40 Gbit/s [4]. The principle of operation is the following: the incoming signal is injected in both arms of the interferometer but time-shifted by τ. Under this condition, the signal induces a phase variation that is suppressed after a time τ by the same signal injected into the second arm. Note that the temporal width of the resulting output pulses is directly controlled by the delay τ.

Finally, one should mention the recent demonstration of standard-mode wavelength conversion at 40 Gbit/s, which uses a newly-designed active-passive SOA-MZI incorporating evanescent-coupling SOAs [5]. The device architecture is moreover flexible in the number of SOAs, thus enabling easier operation optimization and reduced power consumption, leading to simplified architectures and operation for 40 Gbit/s optical 3R regeneration.

2.1.2. Clock-recovery block

Next to the decision, the CR is a second key function in 3R regenerators. One possible approach for CR uses electronics while another uses optics. The first uses OE conversion by means of a photodiode and subsequent EO conversion through a modulator. This conversion becomes more complex and power-hungry as the data-rate increases. It is clear that the maturity of electronics gives a current advantage to this approach. However, considering the pros and cons of electronic CR for cost-effective implementation, the all-optical approach seems more promising, since full regenerator integration is potentially possible with reduced power consumption. In this view, we shall focus here on the optical approach and more specifically on the *self-pulsating effect* in three-sections DFB lasers [6,7]. Results from [8,9] illustrate potentials for high bit rates, broad dynamic range, broad frequency tuning, polarization insensitivity, and relatively short locking times (1 ns). This last feature makes these devices good candidates for operation in asynchronous-packet regime. A 40 Gbit/s loop experiment made possible to assess the recovered optical clock quality and its robustness to long series of consecutive '0' in a transmission system [10]. Another loop demonstration concerned all-optical 10 Gbit/s 3R regeneration, illustrating the technical feasibility of truly all-optical approaches [11].

2.2. Implementation of 40 Gbit/s SOA-MZI-based optical 3R regeneration

As discussed earlier, the nonlinear response is a key parameter for regeneration efficiency. Combining two interferometers is a straightforward means to improve nonlinearity, and hence regeneration efficiency. This approach was first validated at 20 Gbit/s using a cascade of two SOA-MZI [12], see Fig. 5. Such a scheme offers the advantage of restoring data polarity and wavelength, hence making the regenerator inherently transparent. Finally, the second conversion stage can be used as an adaptation interface to the transmission link achieved through chirp tuning in this second device [13].

The device was upgraded to 40 Gbit/s using DOM in both SOA-MZIs (see Fig. 5) with validation in 40 Gbit/s loop transmission [14]. The receiver sensitivity was measured with respect to the number of recirculations or distance at a fixed BER

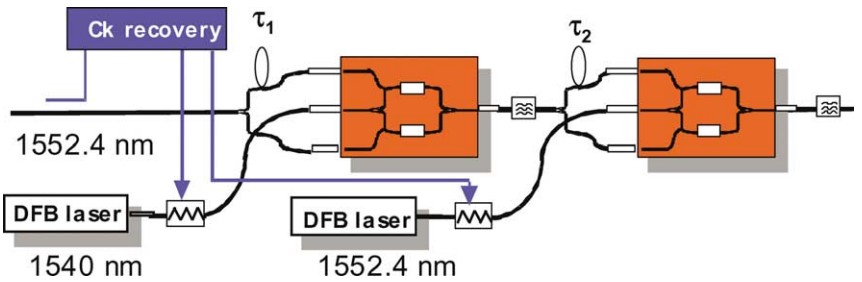

Fig. 5. Optimized structure of a 40 Gbit/s SOA-based 3R regenerator.

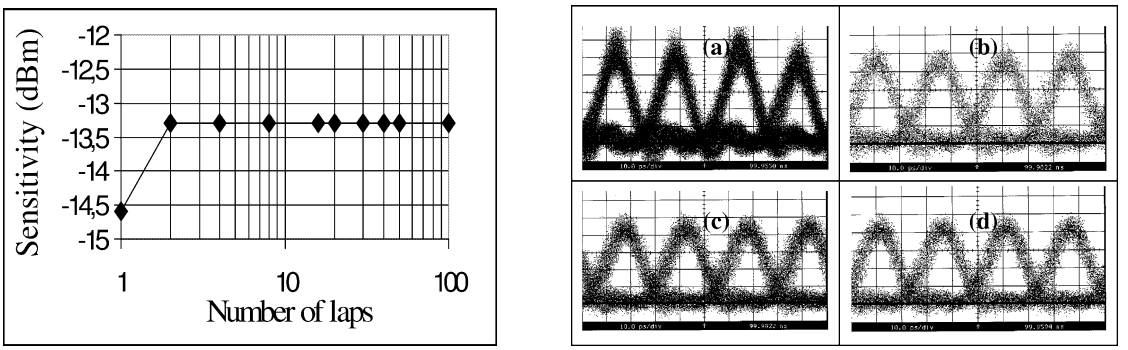

Fig. 6. Evolution sensitivity (left) and 40 Gbit/s eye diagram evolution (right): (a) B-to-B; (b) 1 lap; (c) 10 laps; (d) 100 laps.

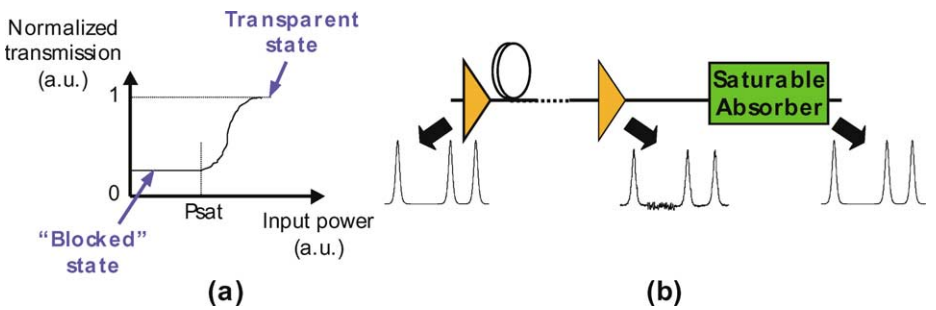

Fig. 7. (a) Saturable Absorber transfer function and (b) Principle of mark/space contrast increase induced by Saturable Absorbers.

of 10^{-9}. Fig. 6 shows the evolution of sensitivity, seen to stabilize to a constant value of -13.3 dBm. The figure also shows the eye diagram monitored at the regenerator output after 1, 10 and 100 circulations. The eye diagram is seen to remain unaltered by distance. Finally, the minimum OSNR tolerated by the regenerator (1 dB sensitivity penalty at 10^{-10} BER) was found to be as low as 25 dB/0.1 nm. These results clearly illustrate the high performance of this SOA-based regenerator structure.

2.3. Optical regeneration by saturable absorbers

We consider next saturable absorbers (SA) as nonlinear elements for optical regeneration. Fig. 8 shows a typical SA transfer function and illustrates the principle of operation. When illuminated with an optical signal with peak power below some threshold (P_{sat}), the photonic absorption of the SA is high and the device is opaque to the signal (low transmittance). Above P_{sat}, the SA transmittance rapidly increases and asymptotically saturates to transparency (passive loss being overlooked). Such a nonlinear transfer function only applies to 2R optical regeneration.

The regenerative properties of SA make possible to reduce cumulated amplified spontaneous emission (ASE) in the '0' bits, resulting in higher contrast between mark and space, hence increasing system performance (Fig. 7(b)). Yet, SAs do not

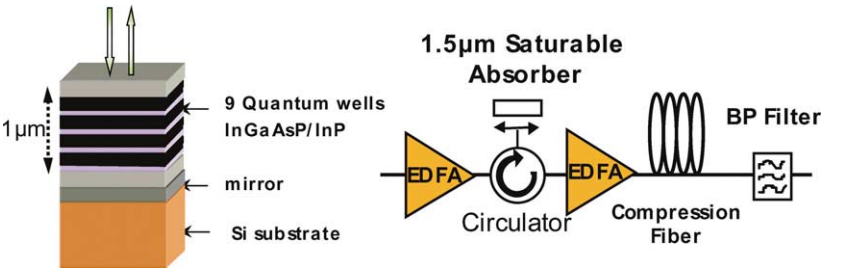

Fig. 8. Structure of Multi-Quantum Well Saturable Absorber (left); 40 Gbit/s-compatible Optical 2R regenerator based on SA (Saturable Absorber) (right).

suppress intensity noise in the marks, which makes the regenerator incomplete. A solution for this noise suppression is *optical filtering* with *nonlinear (soliton) pulses*. The principle is as follows. In absence of chirp, the soliton temporal width scales like the reciprocal of its spectral width (Fourier-transform limit) times its intensity (fundamental soliton relation). Thus, an increase in pulse intensity corresponds to both time narrowing and spectral broadening. Conversely, a decrease in pulse intensity corresponds to time broadening and spectral narrowing. Thus, the filter causes higher loss when intensity increases, and lower loss when intensity decreases. The filter thus acts as an automatic power control (APC) in feed-forward mode, which causes power stabilization. The resulting 2R regenerator (composed by the SA and the optical filter) is fully passive, which is of high interest for submarine systems where the power consumption must be minimal, but it does not include any control in the time domain (no Re-timing).

Different technologies for implementing SAs are available. One possibility is based on the NOLM [15], as described above. However, the most promising approach uses semiconductors. In this case, SA relies upon the control of carrier dynamics through the material's recombination centers. Parameters such as on-off contrast (ratio of transmittance at high and low incident powers), recovery time $(1/e)$ and saturation energy are key to device optimization. Solutions such as *low-temperature-grown* (LTG) *strained multi-quantum wells* (MQW) [16] and ion irradiation of MQW structures [17] were investigated. In the following, we consider a newly-developed ion-irradiated MQW-based device incorporated in a micro-cavity and shown on Fig. 8 [18]. The device operates as a reflection-mode vertical cavity, providing both a high on/off extinction ratio by canceling reflection at low intensity and a low saturation energy of 2 pJ. It is also intrinsically polarization-insensitive. Heavy ion-irradiation of the SA ensures recovery times shorter than 5 ps.

As mentioned above, SAs can be associated with optical filters to ensure efficient and cost-effective optical 2R regeneration, as first demonstrated in 20 Gbit/s transmission [19]. Implementation with 160 km loop periodicity made possible to double the error-free distance ($Q = 15.6$ dB or BER $= 10^{-9}$) of a 20 Gbit/s RZ signal. This result illustrates the capability of the device to reduce noise accumulation at this bit rate or to increase transmission distances in OSNR-limited systems.

To extend the capability of passive 2R regeneration to 40 Gbit/s systems, one can insert a compression fiber between the SA device and the optical filter, as shown in Fig. 8 [20]. Such an improved configuration was experimentally demonstrated in a 40 Gbit/s WDM-like, dispersion-managed loop transmission with 240 km periodicity [21]. Fig. 8 also shows the experimental Q-factor versus transmission distance. Without the regenerator, Q-factors of 13 dB (BER $< 5 \times 10^{-6}$) and 11.3 dB (BER $< 10^{-4}$) were measured after 1300 km and 1650 km, respectively. With the regenerator, a clear improvement in system performance is observed, yielding a Q-factor of 13 dB at 7600 km distance. It should be noted that the main system limitation at such distances stems from timing jitter accumulation and not amplitude fluctuations, since passive regeneration by SA controls OSNR but not timing position. In order to investigate the regenerator capability in the WDM regime, four 200 GHz-spaced additional channels were launched into the loop (see Fig. 9) to emulate realistic WDM conditions. These extra channels contribute to WDM impairments but are extracted from the loop by the Demux stage in front of the SA. The regenerated channel performance then became $Q = 13$ dB at 2200 km distance and 11.3 dB after 7600 km, which compares well to previous single-channel results. One should also note that such a system performance is fully compatible with FEC to yield error-free, 40 Gbit/s WDM system operation over 7600 km.

Passive optical 2R regeneration is of high interest in long-haul transmission (typically in noise-limited systems) since implementation of SA increases the system's robustness to OSNR degradation without any extra power consumption. Reducing both saturation energy and insertion loss along with increasing dynamic contrast represent key future device improvements. Regeneration of WDM signals from the same device such as one SA chip with multiple fibers [22] implemented between MUX/DMUX stages should also be thoroughly investigated. In this respect, SA wavelength selectivity in *quantum dots* [23] could be advantageously exploited.

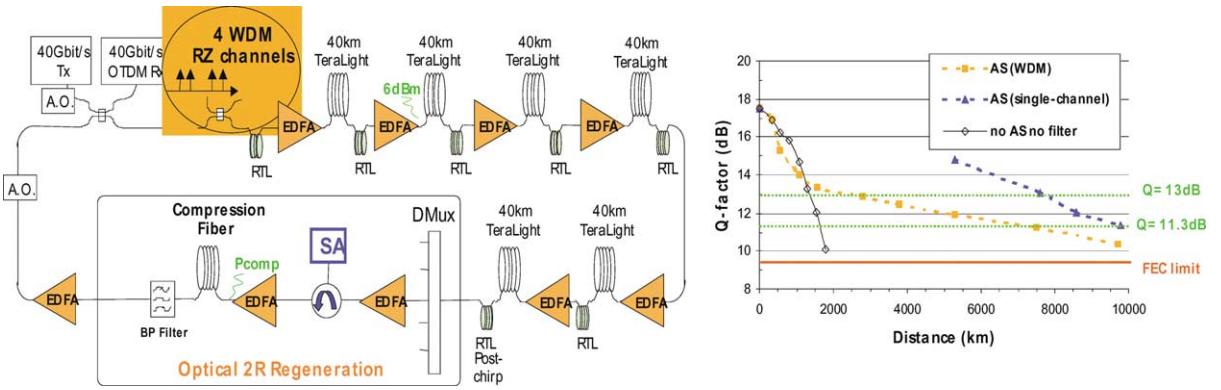

Fig. 9. Experimental loop set-up for 40 Gbit/s long-haul transmissions (left); SA (Saturable Absorber); Experimental Q-factor evolution with transmission distance (right).

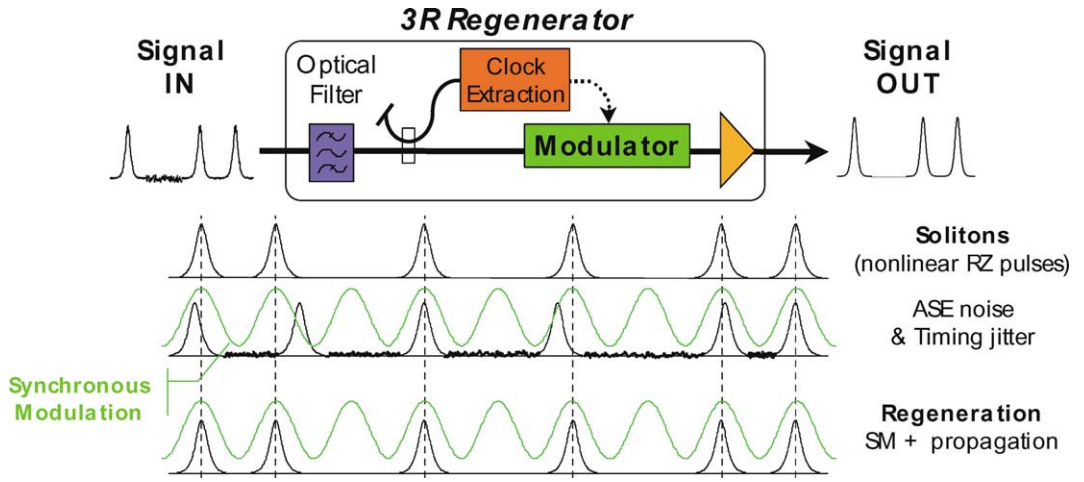

Fig. 10. Basic layout of the all-optical regenerator by synchronous modulation and narrowband filtering and illustration of the principle of operation.

3. Optical 3R regeneration by synchronous modulation

3.1. Principle of operation

All-optical 3R regeneration can be achieved through *in-line synchronous modulation* (SM) associated with narrowband filtering (NF) [24]. Modulation can be made on either signal intensity (IM) or phase (PM) [25], or a combination of both [26]. As shown in Fig. 10, the layout of the SM regenerator is straightforward. It includes a CR block, a modulator and an optical filter. Regeneration through SM-NF intrinsically requires nonlinear (soliton) propagation in the trunk fiber following the SM block. Therefore, one can refer to the approach as *distributed optical regeneration*. This contrasts with *lumped regeneration*, where 3R is completed within the regenerator, and is independent of line transmission characteristics. As discussed below, it is yet possible to make the regeneration function and transmission work independently in such a way that *any* type of RZ signals (soliton or non-soliton) can be transmitted through the system. We refer to this approach as *'black box' optical regeneration* (BBOR) [27].

The control effects of IM and PM over optical pulses are qualitatively different. Both IM and PM reduce timing jitter regardless its physical *origin* (Gordon–Haus, XPM, pulse-to-pulse interactions or PMD-induced jitter). However, jitter reduction through PM relies on a time-position-dependent frequency shift of the RZ pulses, resulting in velocity changes due to chromatic dispersion, while jitter suppression through IM uses self-forming properties of soliton pulses which induces detrimental energy fluctuations. These can be efficiently controlled by NF, according to the principle previously described. However, only IM makes it possible to remove ASE noise, leading to asymptotic OSNR stabilization and enabling transmission over virtually unlimited

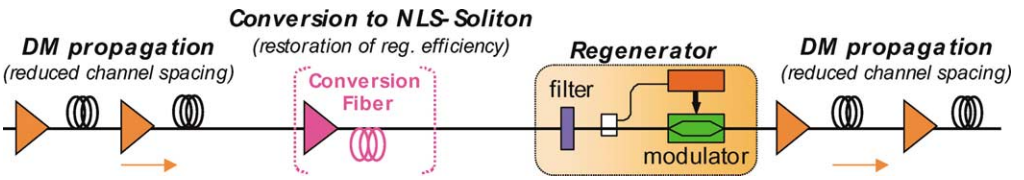

Fig. 11. Schematic of Black-Box Optical Regenerator (BBOR).

distances [24]. In fact, distance is not a limiting parameter in optically-regenerated systems, unlike in the conventional OE case. All loop experiments for 40 Gbit/s SM-NF-based regeneration concern measured distances over 10 000 km [28–30].

One should note that SM-NF regeneration requires soliton-like pulses, without which time and intensity noise cannot be controlled. This requirement is of major import for transmission line design: regeneration and transmission *cannot* be designed independently from each other. As discussed next, however, it is possible to separate these two functions in such a way that the transmission line characteristics can be chosen/designed independently from that of the SM-NF regenerator.

3.2. The Black-Box Optical Regenerator (BBOR) approach

In the previous section, SM-NF-based regeneration was shown to work on solitons pulses, which links the regenerator and the line system designs. We show here that the black-box optical regeneration (BBOR) makes it possible to separate the two. One can then independently exploit *dispersion management* (DM) techniques for increasing spectral efficiency in long-haul transmission, while ensuring high transmission quality through BBOR.

The BBOR technique consists to include an adaptation stage for incoming RZ pulses in the SM-based regenerator, which ensures high regeneration efficiency regardless of RZ signal format (linear RZ, DM-soliton, C-RZ, etc.). This is achieved using a local and periodic soliton conversion of RZ pulses by means of launching an adequate power into some length of fiber with anomalous dispersion. Fig. 11 shows the BBOR structure enabling the successful association of DM propagation and SM regeneration by SM [27]. The actual experimental demonstration of the BBOR approach and its superiority over the 'classical' SM-based scheme for DM transmission was experimentally investigated in 40 Gbit/s DM loop transmission [31].

The BBOR can permit significant increases in *information spectral density* (ISD). In [32], a 32×40 Gbit/s BBOR-transmission with 150 GHz channel spacing (0.3 bit/s/Hz ISD) was numerically demonstrated, with asymptotic Q-factors above 19 dB (linear $Q > 8.9$) at 10 000 km distance. This result also demonstrates the feasibility of Tbit/s ($N \times 40$ Gbit/s) transoceanic systems with ISD up to 0.3 bit/s/Hz. The issue of maximizing BBOR spacing along the transmission line was also addressed (as impacting on system complexity, cost, power consumption and overall performance). Current investigations show that regeneration spacings up to 600 km are possible.

Finally, BBOR systems are tolerant to initial pulse shape/format, ranging from short-RZ pulse to 50%-RZ pulses to NRZ [33]. This result could lead to cost-effective simplification of system transceivers with the removal of RZ-shaping stages.

3.3. WDM optical regeneration

Since high-capacity systems are based on WDM, multiple-wavelength optical regeneration is a key issue. In particular, *simultaneous regeneration* of WDM channels through a *single* 3R device would represent considerable added value.

Two possible implementations of optical 3R regeneration with WDM can be conceived. The first (Fig. 12, top) consists in allocating a regenerator to each WDM channel. The second consists in sharing a single modulator, thus processing the WDM channels at once in serial fashion [34]. This approach requires WDM synchronicity, meaning that all bits be synchronous with the modulation. Such WDM synchronicity can be achieved either by use of appropriate time-delay lines located within a DMux/Mux apparatus (Fig. 12, bottom left), or by making the WDM channels inherently time-coincident at specific regenerator locations (Fig. 12, bottom right). This WDM regeneration scheme also implies the regenerator be WDM crosstalk-free, as is the case of EO-InP Mach–Zehnder interferometer [30]. Clearly, serial regeneration scheme is far simpler and cost-effective than the parallel version; however, optimized re-synchronization schemes still remain to be developed for realistic applications.

To investigate the BBOR performance in simultaneous WDM regeneration, a 4×40 Gbit/s DM loop experiment with 1.6 nm channel spacing (ISD = 0.2 bit/s/Hz) was conducted [35]. At 10 000 km, the asymptotic Q-factors of the four channels were measured to be greater than 14.5 dB (5×10^{-8} BER) for $2^{31} - 1$ coding length. The associated system penalty at 10 000 km is only 2 dB compared to previous single-channel 40 Gbit/s measurement [31]. These results also correspond to the very first demonstration of simultaneous 40 Gbit/s WDM regeneration.

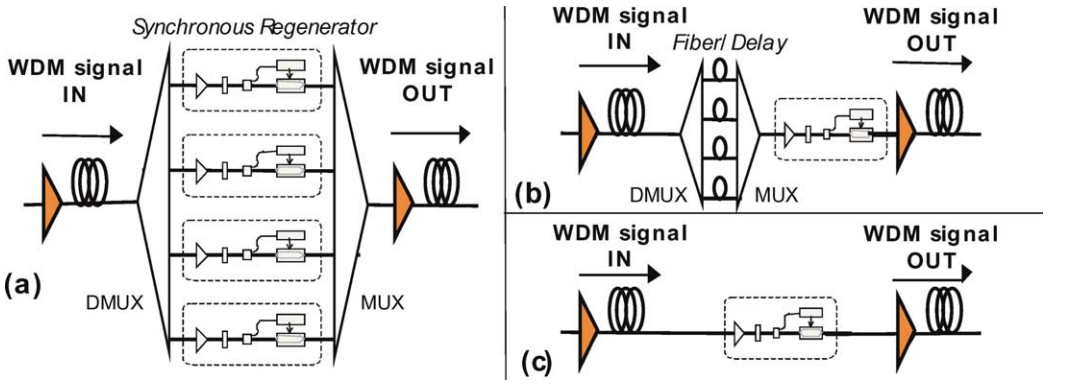

Fig. 12. Basic implementation schemes for WDM all-Optical Regeneration: (a) parallel asynchronous; (b) serial re-synchronized; and (c) serial self-synchronized.

4. Electro-optical vs. all-optical 3R regeneration

After having described the current status and trends on all-optical regeneration, two key questions remain. Is this technology the only solution for increasing capacity or transmission distance? Secondly, at which data rate and WDM granularity would signal regeneration be required and in what system or network type?

Consider the first question. Should one accept further system complexity, then OE regeneration should not be overlooked. In fact, the circuitry of OE repeater/regenerators is broadband and its integration from the input photodiode to the output laser driver is very complex. A parallel, channel-by-channel implementation (apparently the only possibility) amounts to building two complete WDM terminal equipments in a back-to-back configuration. For long-haul systems such as submarine ones, WDM terminal concatenation throughout the trunk is a solution technically possible, but it makes no economical sense. On the other hand, optical regenerators are significantly simpler. In contrast with OE regeneration, the only high-speed electronics involved is narrowband (SM- or/and SOA-MZI-based regenerators), which reduces RF circuitry complexity and power consumption. Moreover, complete integration (with either OE or all-optical CR) of parallel optical modulators onto a single semiconductor chip is technologically feasible. In the case of medium-haul systems and terrestrial networks, both approaches of parallel OE and all-optical regenerations are technically sound, due to additional requirements for add-drop multiplexing, switching and network protection. In this case, the choice between electronic and optical solutions must be guided by system architecture and cost considerations.

5. Conclusion

We have reviewed the current status of all-optical regeneration technologies, which have promising potential for future high bit-rate systems. A variety of solutions was described, including saturable absorbers, nonlinear interferometer/gates and synchronous modulators. Operating at 40 Gbit/s, these solutions correspond to a vast array of possibilities, all having potential for dense/compact integration and hence reduced operational cost. While in-line optical regeneration clearly represents a key alternative for future progress in long-haul transmission, several technical and economical issues remain to be addressed for practical/industrial implementation.

From the technical side, a workable solution for optical regeneration should include all aspects of system engineering, from power consumption issues to packaging issues. A 3R regenerator is in itself a subsystem, which implies a high level of reliability, with enhanced supervision and monitoring requirements. Conceptually, regenerators should accept *any* number of WDM channels. As highlighted in this article, all-optical regeneration offers a unique possibility for simultaneous regeneration of WDM channels, as opposed to the classical OE approach. However, this requires WDM channel re-synchronization and that all channels have identical transmitter clocks. These issues being eventually solved, there will remain a problem of power-handling limit for the regenerator.

From the economics side, the challenges of all-optical regeneration are not specifically different from those concerning new telecom technologies: performance enhancements are measured in $-per-wavelength and time-to-market figures. Albeit the added value of optical regeneration is tangible for point-point links, its merits in optical networking have been barely considered and remain to be put in perspective.

From today's status concerning the two alternative approaches for in-line regeneration (OE or all-optical), it is safe to say that the choice between either solution will be primarily dictated by both engineering and economical considerations. It will

result from a tradeoff between overall system performance, system complexity and reliability, availability, time-to-market and rapid returns from the technology investment.

References

[1] P. Öhlén, E. Berglind, IEEE Photon. Technol. Lett. 9 (7) (1997).
[2] S. Bigo, O. Leclerc, E. Desurvire, IEEE J. Selected Topics Quantum Electron. 3 (5) (1997) 1208–1223.
[3] T. Durhuus, B. Mikkelsen, C. Joergensen, S.L. Danielsen, K.E. Stubkjaer, J. Ligthwave Technol. 14 (6) (1996).
[4] S. Fischer, M. Dülk, E. Gamper, W. Vogt, E. Gini, H. Melchior, W. Hunziker, D. Nesset, A.D. Ellis, Electron. Lett. 35 (23) (1999).
[5] B. Dagens, A. Labrousse, S. Fabre, B. Martin, S. Squedin, B. Lavigne, R. Brenot, M.L. Nielsen, M. Renaud, in: Proc. European Conference on Optical Communications, ECOC '02, Copenhague, Denmark, 2002, Paper PD 3.1.
[6] B. Sartorius, M. Möhrle, S. Reichenbacher, H. Preir, H.J. Wünsche, U. Bandelow, IEEE J. Quantum Electron. 33 (2) (1997).
[7] S. Bauer, O. Brox, J. Sieber, M. Wolfrum, Novel concept for a tunable optical microwave source, in: Proc. Conference on Optical Communications, OFC '2002, Optical Society of America, Washington, DC, 2002, p. 478, paper ThM5.
[8] C. Bornholdt, B. Sartorius, M. Möhrle, in: Proc. European Conference on Optical Communications, ECOC '99, Nice, France, 1999, p. 54, post deadline paper PD 3-5.
[9] D. Chiaroni, B. Lavigne, A. Dupas, P. Guerber, A. Jourdan, F. Devaux, C. Bornholdt, S. Bauer, B. Sartorius, M. Mörhle, in: Proc. of European Conference on Optical Communications, ECOC '2000, Vol. 4, Munich, Germany, 2000, p. 69, paper 10.4.5.
[10] B. Sartorius, C. Bornholdt, S. Bauer, M. Mörhrle, P. Brindel, O. Leclerc, in: Proc. Conference on Optical Communications, OFC '2000, Optical Society of America, Washington, DC, 2000, post-deadline paper PD11.
[11] B. Lavigne, P. Guerber, D. Chiaroni, C. Janz, A. Jourdan, B. Sartorius, C. Bornholdt, M. Mörhle, in: Proc. of European Conference on Optical Communications, ECOC '99, Vol. 2, Nice, France, 1999, p. 262, paper ThA2-3.
[12] B. Lavigne, P. Guerber, C. Janz, A. Jourdan, M. Renaud, in: Proc. Conference on Optical Communications, OFC '2000, Vol. 4, Optical Society of America, Washington, DC, 2000, p. 93, paper ThF7.
[13] P. Guerber, B. Lavigne, C. Janz, A. Jourdan, D. Wolson, T. Fjelde, A. Kloch, in: Proc. European Conference on Optical Communications, ECOC '2000, Vol. 3, Munich, Germany, 2000, p. 121, paper 8.4.3.
[14] B. Lavigne, P. Guerber, P. Brindel, E. Balmefrezol, B. Dagens, in: Proc. European Conference on Optical Communications, ECOC '2001, Vol. 3, Amsterdam, Netherlands, 2001, p. 290, paper We.F. 2.6.
[15] N.J. Doran, D. Wood, Opt. Lett. 13 (1) (1988) 5658.
[16] R. Takahashi, Y. Kawamura, H. Iwamura, in: Proc. European Conference on Optical Communications, ECOC '94, Vol. 1, Firenze, Italy, 1994, pp. 113–115;
R. Takahashi, Y. Kawamura, T. Kagawa, H. Iwamura, Appl. Phys. Lett. 65 (14) (1994) 1790–1792.
[17] E. Lugagne-Delpon, J.-L. Oudar, N. Bouché, R. Raj, A. Shen, N. Stelmakh, J.-M. Lourtioz, Appl. Phys. Lett. 72 (7) (1998) 759–761.
[18] J. Mangeney, G. Aubin, J.-L. Oudar, J.-C. Harmand, G. Patriache, H. Choumane, N. Stelmakh, J.-M. Lourtioz, Electron. Lett. 36 (17) (2000) 1486.
[19] O. Leclerc, G. Aubin, P. Brindel, J. Mangeney, H. Choumane, S. Barré, J.-L. Oudar, Electron. Lett. 36 (23) (2000) 1944.
[20] M. Matsumoto, O. Leclerc, Electron. Lett. 38 (12) (2002) 576.
[21] D. Rouvillain, F. Seguineau, L. Pierre, P. Brindel, H. Choumane, G. Aubin, J.-L. Oudar, O. Leclerc, in: Proc. Conference on Optical Communications, OFC '2002, Optical Society of America, Washington, DC, 2002, post-deadline paper FD11.
[22] A. Shen, M. Goix, S. Louis, D. Delagrandière, J. Decobert, G. Hénin, D. Rouvillain, O. Leclerc, H. Choumane, G. Aubin, J.-L. Oudar, in: Proc. European Conference on Optical Communications, ECOC '02, Vol. 2, Copenhagen, Denmark, 2002, paper 5.4.5.
[23] T. Akiyama, H. Kuwatsuka, T. Simoyama, Y. Nakata, K. Mukai, M. Suguwara, O. Wada, H. Ishikawa, in: Proc. European Conference on Optical Communications, ECOC '2000, Munich, Germany, 2000, p. 291, paper 9.3.6.
[24] M. Nakazawa, E. Yamada, H. Kubota, K. Suzuki, Electron. Lett. 27 (14) (1991) 1270.
[25] N.J. Smith, K.J. Blow, W.J. Firth, K. Smith, Opt. Commun. 102 (1993) 324.
[26] O. Leclerc, E. Desurvire, O. Audouin, Electron. Lett. 32 (12) (1996).
[27] P. Brindel, B. Dany, O. Leclerc, E. Desurvire, Electron. Lett. 35 (6) (1999) 480–481.
[28] G. Aubin, T. Montalant, J. Moulu, F. Pirio, J.-B. Thomine, F. Devaux, Electron. Lett. 32 (24) (1996) 2188.
[29] K. Suzuki, H. Kubota, A. Sahara, M. Nakazawa, Electron. Lett. 34 (1) (1998) 98.
[30] O. Leclerc, P. Brindel, D. Rouvillain, E. Pincemin, B. Dany, E. Desurvire, C. Duchet, E. Boucherez, S. Bouchoule, Electron. Lett. 35 (9) (1999) 730–731.
[31] B. Dany, P. Brindel, E. Pincemin, D. Rouvillain, O. Leclerc, Opt. Lett. 25 (11) (2000) 793–795.
[32] O. Leclerc, P. Brindel, B. Dany, F. Devaux, C. Duchet, L. Fleury, P. Nouchi, D. Rouvillain, A. Shen, in: Proc. Conference SubOptic '01, Vol. 1, Kyoto, 2001, p. 229, paper 3.1.5.
[33] O. Leclerc, B. Lavigne, D. Chiaroni, E. Desurvire, in: Kaminow, Li (Eds.), Optical Fiber Technologies IVA, Academic Press, San Diego, 2002, Chapter 15.
[34] E. Desurvire, O. Leclerc, O. Audouin, Opt. Lett. 21 (14) (1996) 1026–1028.
[35] O. Leclerc, B. Dany, D. Rouvillain, P. Brindel, E. Desurvire, C. Duchet, A. Shen, F. Devaux, A. Coquelin, M. Goix, S. Bouchoule, L. Fleury, P. Nouchi, Electron. Lett. 36 (18) (2000) 1574.